Development of an elastoplastic constitutive model in the framework of the multilaminate method for numerical analyses of geotechnical structures

Mohammad Falahatpour[a], Mohammad Oliaei[b*], and Heisam Heidarzadeh[c]

[a] PhD. Candidate in Geotechnic, Department of Civil Engineering, Tarbiat Modares University, Tehran, Iran (E-mail: m.falahatpour@modares.ac.ir)

[b] Assistant Professor, Department of Civil Engineering, Tarbiat Modares University, Tehran, Iran (E-mail: m.olyaei@modares.ac.ir)

[c] Associate Professor, Department of Civil Engineering, Faculty of Technology and Engineering, Shahrekord University, Shahrekord, Iran (E-mail: Heidarzadeh@sku.ac.ir)

Abstract

In this study, a generalized constitutive model, in which the yield and potential plastic surfaces do not need to be explicitly defined, is presented in the framework of the multilaminate method. In this framework, the constitutive relations are defined as the relationship between volumetric and deviatoric stresses and strains on several planes in different directions, called microplane. A new volumetric- deviatoric stress space is defined on the microplane, which has a volumetric component similar to the definition of mean stress. However, the deviatoric component is defined as the resultant of a normal deviatoric component and two shear components on the microplane. The use of the new innovative stress space facilitates the application of volumetric- deviatoric based constitutive models in the multilaminate framework. The results of the model for several types of clay and sand in drained and undrained conditions have been validated with experimental data and results presented by similar models and it was observed that the proposed model, in addition to the simplicity of the formulation, can correctly predict the behavior of sand and clay materials in different conditions.

KEYWORDS: Multilaminate, Microplane, Generalized plasticity, Elastoplastic, Constitutive model, Stress space

1. Introduction

The multi-plane theory has been used by many researchers. This framework was used by Zienkiewicz and Pande[1] to predict the behavior of jointed rocks. Also, Pande and Sharma[2] presented an elastoplastic model in clays based on the multilaminate theory. They numerically estimated the effect of rotation of the principal axes on volumetric and deviatoric plastic strains. Shiomi and Pietruszczak[3] used another elastoplastic model called the reflecting surface to predict the liquefaction of sand layers, in which the behavior of sand under isotropic conditions was predictable without considering the imposed anisotropy in the plastic strain process. Bažant and Oh[4] expanded the scope of this theory to the analysis of the fracture of concrete structures by providing a model called the microplane model. Another elastoplastic model based on multilaminate theory was presented by Sadrnejad and Pande[5] to predict sand behavior. Sadrnejad et al.[6] Presented a Multi-Line constitutive model using a multilaminate model for granular soils. Zreid and Kaliske[7] presented a microplane plasticity model based on the Drucker-Praeger yield criterion. Dashti et al.[8] used the constitutive model presented by Dafalias and Manzari[9] in the framework of a multilaminate model to simulate sand liquefaction. Malisetty et al.[10] presented a model using a multilaminate framework based on generalized plasticity and associated critical state concepts to describe the mechanical behavior of granular materials. Many other researches have been done on multilaminate models, such as[11–16].

In the literature, different stress spaces have been used on microplanes: Dashti et al.[17,18] have used the stress ratio space on the π plane. There are three components on the deviatoric plane (π plane), which are the ratio of deviatoric stresses to normal stress. In some researches[10,12,19–22], the normal stress-shear stress space is used. Bayraktaroglu et al.[23] used the space of normal stress-shear stress, where normal stress consists of two components, volumetric and deviatoric. Bažant et al.[24] has used the stress space of volumetric- normal deviatoric-shear stress. Caner et al.[25] has used the stress space in terms of volumetric and deviatoric components of normal stress and two shear components. Cudny and Vermeer[26] have used a normal stress-shear stress space and used a yield surface whose cap part is according to Modified Cam Clay model. Since the stress space of shear stress-normal

* Corresponding author. Tel.: +98 2182884395, Mobile: +989122107442 E-mail addresses: m.olyaei@modares.ac.ir

stress is suitable for constitutive models similar to Mohr-Coulomb and for models developed in $p-q$ space such as Modified Cam Clay, it is better to use a stress space similar to $p-q$ on microplanes. Therefore, choosing a simple stress space compatible with the constitutive model that used on the microplane is necessary.

In this article, a new volumetric- deviatoric stress space is presented on the microplanes, in which constitutive relations can be written algebraically and this simplifies calculations and increases the speed of analysis. Then, a generalized plasticity constitutive model is written in this new stress space, which can predict the behavior of sands and clays well.

2. Multilaminate framework

The basis of the multilaminate theory is to determine the numerical relationship between the two states of interparticle behavior (microscale behavior) and engineering mechanical properties (large-scale behavior) in the form of a constitutive equation. In other words, in this case, the material properties are obtained according to each of its components; and it could be possible to achieve the stress-strain relation of the soil by studying the interparticle behavior[6].

As known, soil materials are composed of an unlimited number of solid particles that interact with each other. The reaction between the particles is due to the contact force during their contact. The analysis of the behavior of the particles and their contact surfaces depends on the number, size, shape, roughness, and strength of the particles at these surfaces. Therefore, this approach is much more complex than assuming a continuous environment. On the other hand, in a simple approach, the behavior of the soil can be assumed to be a combination of the elastic behavior of the grains and the plastic slip at the boundaries between the grains. Thus, in an artificial state, the three-dimensional behavior of soil materials can be explained by considering the numerous sample planes on which slipping occurs. These planes divide the soil mass into a set of polygonal pieces next to each other. In this case, similar to the slipping of real soil grains, slipping and deformation perpendicular to the contact planes of different parts is the basic method of creating a plastic strain[27].

2-1 Numerical concept of multilaminate theory

The classical constitutive models represent invariant equations that directly relate σ_{ij} and ε_{ij} to the components of the stress and strain tensors σ and ε (the Latin indices refer to the Cartesian coordinate components x_i ; $i=1,2,3$). A multilaminate constitutive model is defined by the relationship between stresses and strains applied to the plane. These planes are called microplane and have an arbitrary orientation that is denoted by its normal unit vector n_i [27].

The basis of this theory is the calculation of the numerical integration of a given mathematical function developed over a sphere surface having a radius of one. This mathematical function can express changes in physical properties at the sphere surface. The surface of a hypothetical sphere in numerical integration can be approximated by numerous numbers of flat planes that are tangent to different points of the sphere surface. Thus, each of the mentioned planes has a point of contact with the surface of the sphere; by limiting the number of these planes, the number of contact points or reference points can be defined, and in calculating the numerical integral, the value of the quantity spread on the surface of the sphere can be obtained at the points mentioned. Numerical integrals are obtained from the continuous function $f(x,y,z)$ on the sphere's surface as the sum of the values of f at the reference points multiplied by the weight coefficients corresponding to these points. The number of sample points should be increased to decrease the error. In this case, it is proved that the application of *34* reference points reduces the error sufficiently[8]. According to symmetry, a hemisphere with *17* planes can be considered. Figure 1(a) shows the position of *34* points and the planes tangent to them, and Figure 1(b) shows the simulated shape of a sphere with planes for numerical integration.

The relationship between the numerical integration and the ordinary integral is obtained as follows:

$$\int_A f(x,y,z)\,dA = \sum_{\mu=1}^{\mu_N} f_\mu\left(x_\mu, y_\mu, z_\mu\right) dA_\mu \qquad (1)$$

$$W_\mu = \frac{A_\mu}{A} \quad , \quad A = 4\pi \tag{2}$$

According to Eq (1) and Eq. (2) we have:

$$\int_A f(x,y,z)\,dA = 4\pi \sum_{\mu=1}^{\mu_N} W_\mu f_\mu\left(x_\mu, y_\mu, z_\mu\right) \tag{3}$$

in which, A is the surface of the sphere, N is the number of points, W_μ is the weight coefficient of the point μ , and $f_\mu\left(x_\mu, y_\mu, z_\mu\right)$ is the value of the function f at the point μ . In this way, any change that occurs on the plane μ is related to the point μ . A plane is defined for each point in such a way that the direction cosines of the contact points are the same direction cosines perpendicular to the plane[6,20].

The basic hypothesis is that the strain vector $\vec{\varepsilon}_N$ on the microplane (Figure 2) is the image ε , meaning $\varepsilon_{N_i} = \varepsilon_{ij} n_j$. The normal strain on the plane is equal to $\varepsilon_N = n_j \varepsilon_{N_i}$. It could be written as follows:

$$\varepsilon_N = N_{ij} \varepsilon_{ij} \tag{4}$$

Where $N_{ij} = n_i n_j$ (repetition of subscripts referring to Cartesian coordinates x_{ii} , means summation over $i = 1,2,3$).

The shear strains on each microplane are determined by their components in the M and L directions given by orthogonal unit coordinate vectors $\vec{m}$ and $\vec{l}$, shown by components m_i and l_i laying within the microplane. The vector m_i can, for example, be selected perpendicular to the x_3 axis, in which case $m_1 = n_2\left(n_1^2 + n_2^2\right)^{-1/2}$, $m_2 = -n_1\left(n_1^2 + n_2^2\right)^{-1/2}$ and $m_3 = 0$, but $m_1 = 1$ and $m_2 = m_3 = 0$ if $n_1 = n_2 = 0$. A vector m_i perpendicular to x_1 or x_2 can be obtained by converting the indices $1, 2$ and 3 . The orthogonal unit vector is created as $\vec{l} = \vec{m} \times \vec{n}$. The components of shear strain in the directions of $\vec{m}$ and $\vec{l}$ are equal to $\varepsilon_M = m_i\left(\varepsilon_{ij} n_j\right)$ and $\varepsilon_L = l_i\left(\varepsilon_{ij} n_j\right)$, and with the symmetry property of the tensor ε_{ij}

$$\varepsilon_M = M_{ij} \varepsilon_{ij} \quad , \quad \varepsilon_L = L_{ij} \varepsilon_{ij} \tag{5}$$

Where $M_{ij} = \left(m_i n_j + m_j n_i\right)/2$ and $L_{ij} = \left(l_i n_j + l_j n_i\right)/2$ [28,29].

The direction cosines of these 17 planes with their weight coefficients are shown in

Table 1.

Due to the kinematic constraint that relates the strains at the microlevel (microplane) and the macrolevel (continuum medium), the static equivalence (equilibrium) between the macro and micro levels can be applied only approximately. It is done by the principle of virtual work[30] written for the surface Ω of a unit hemisphere.

$$\frac{2\pi}{3} \sigma_{ij} \delta\varepsilon_{ij} = \int_\Omega \left(\sigma_N \delta\varepsilon_N + \sigma_M \delta\varepsilon_M + \sigma_L \delta\varepsilon_L\right) d\Omega \tag{6}$$

This equation means that the virtual work of macro stresses (continuum stresses) on a unit sphere must be equal to the virtual work of micro stresses (microplane stress components) considered as traction on the surface of the sphere. The integral physically represents the homogenization of different contributions coming from planes with different orientations within the material, as shown in Figure 1(a) (for further physical justification, see[31]).

Substituting $\delta\varepsilon_N = N_{ij} \delta\varepsilon_{ij}$, $\delta\varepsilon_M = M_{ij} \delta\varepsilon_{ij}$ and $\delta\varepsilon_L = L_{ij} \delta\varepsilon_{ij}$, and given that the last parametric equation must be held for each change $\delta\varepsilon_{ij}$ the following fundamental equilibrium relation is obtained[30]:

$$\sigma_{ij} = \frac{3}{2\pi}\int_{\Omega} S_{ij} d\Omega \quad \approx \quad 6\sum_{\mu=1}^{\mu_w} w_\mu S_{ij}^{(\mu)}$$
$$S_{ij} = \sigma_N N_{ij} + \sigma_M M_{ij} + \sigma_L L_{ij} \tag{7}$$

As shown, the integral in numerical calculations is approximated by an optimal Gaussian integration formula for a spherical surface[32,33], which represents the weighted sum on micro-planes with orientation η_μ; the weights w_μ are normalized so that $\sum w_\mu = 1/2$ [32,34]. In the finite element analyses, integral (7) must be calculated at each point of integration of each finite element in each time step. The values of the direction cosines for all the microplanes are common to all the integration points for all the finite elements and are pre-calculated and stored.

2-2 Application of multilaminate theory in constitutive modeling

The most general explicit constitutive relationship in the multilaminate area can be written as follows:

$$\begin{aligned} \sigma_N &= \mathcal{F}^t\left[\varepsilon_N, \varepsilon_M, \varepsilon_L\right] \\ \sigma_M &= \mathcal{G}^t\left[\varepsilon_N, \varepsilon_M, \varepsilon_L\right] \\ \sigma_L &= \mathcal{H}^t\left[\varepsilon_N, \varepsilon_M, \varepsilon_L\right] \end{aligned} \tag{8}$$

where $\mathcal{F}, \mathcal{G}$ and $\mathcal{H}$ are functions of the strain history of the microplanes at time t.

The normal strain component on microplanes consists of two parts, volumetric and deviatoric.

$$\varepsilon_N = \varepsilon_D + \varepsilon_V \quad , \quad \varepsilon_v = \varepsilon_{kk}/3 \tag{9}$$

The volumetric strain (mean strain) is the same for all microplanes. Work-conjugate volumetric stress is used to obtain normal volumetric and deviatoric components of stress on microplanes. Therefore, the volumetric stress on the microplanes is defined by the following equation.

$$\frac{2\pi}{3}\frac{\sigma_{kk}}{3}\delta\varepsilon_{mm} = \int_{\Omega}\left(\sigma_V \delta\varepsilon_V\right) d\Omega \tag{10}$$

By substituting $\varepsilon_V = \varepsilon_{kk}/3$ and considering $\int_{\Omega} d\Omega = 2\pi$ for volumetric stress on the microplanes the following relation will be obtained

$$\sigma_V = \sigma_{kk}/3 \tag{11}$$

Subtracting the Equation (10) from (6):

$$\frac{2\pi}{3}\left(\sigma_{ij} - \frac{\sigma_{kk}}{3}\delta_{ij}\right)\delta\varepsilon_{ij} = \int_{\Omega}\left(\sigma_D\delta\varepsilon_D + \sigma_D\delta\varepsilon_V + \sigma_V\delta\varepsilon_D + \sigma_M\delta\varepsilon_M + \sigma_L\delta\varepsilon_L\right) d\Omega \tag{12}$$

where $\sigma_D = \sigma_N - \sigma_V$ and $\delta\varepsilon_D = \delta\varepsilon_N - \delta\varepsilon_V$. Noting that the deviatoric stress tensor $\sigma_{ij}^D = \sigma_{ij} - \left(\sigma_{kk}/3\right)\delta_{ij}$, and that $\int_{\Omega}\sigma_D\delta\varepsilon_V d\Omega = \int_{\Omega}\sigma_V\delta\varepsilon_D d\Omega = 0$, we have

$$\sigma_{ij}^D\delta\varepsilon_{ij} = \frac{2\pi}{3}\int_{\Omega}\left(\sigma_D\delta\varepsilon_D + \sigma_M\delta\varepsilon_M + \sigma_L\delta\varepsilon_L\right) d\Omega \tag{13}$$

Kinematic constraint means that the micro-strains (components of the strain tensor on the microplanes) are calculated as the strain tensor image (macro strains). Therefore, we have $\delta\varepsilon_N = N_{ij}\delta\varepsilon_{ij}$ results $\delta\varepsilon_D = \delta\varepsilon_N - \delta\varepsilon_V = \left(N_{ij} - \delta_{ij}/3\right)\delta\varepsilon_{ij}$ and $\delta\varepsilon_M = M_{ij}\delta\varepsilon_{ij}$ with $\delta\varepsilon_L = L_{ij}\delta\varepsilon_{ij}$. By substituting these relations in Equation (13) the following result is obtained.

$$\begin{aligned} \sigma_{ij} &= \sigma_{ij}^D + \sigma_V\delta_{ij} \\ \sigma_{ij}^D &= \frac{3}{2\pi}\int_{\Omega}\left[\sigma_D\left(N_{ij} - \frac{\delta_{ij}}{3}\right) + \sigma_M M_{ij} + \sigma_L L_{ij}\right] d\Omega \end{aligned} \tag{14}$$

By volumetric-deviatoric separation, elastic stress-strain relationships of microplanes can be written in the rate form as follows

$$\begin{aligned}\dot{\sigma}_V &= E_V\dot{\varepsilon}_V\\ \dot{\sigma}_D &= E_D\dot{\varepsilon}_D\\ \dot{\sigma}_M &= E_T\dot{\varepsilon}_M\\ \dot{\sigma}_L &= E_T\dot{\varepsilon}_L\end{aligned} \tag{15}$$

Where E_V, E_D and E_T are the elastic modulus of the microplanes and their relation to the macroscopic modulus of Young (E) and the Poisson ratio (ν) is equal to $E_V = E/(1-2\nu)$, $E_D = 5E/\left[(2+3\lambda)(1+\nu)\right]$ and $E_T = \lambda E_D$ [28,29]. Here, λ is a parameter to be selected and the best choice is $\lambda = 1$[31]. By choosing $\lambda = 1$and according to the macroscopic shear and volume modulus:

$$\begin{aligned}E_V &= 3K_{ev}\\ E_D &= E_T = 2G_{es}\end{aligned} \tag{16}$$

where $K_{ev} = K_{ev0}\left(p'/p_0\right)$and $G_{es} = G_{es0}\left(p'/p_0\right)$ [35]. Now, to define a generalized plasticity constitutive model on microplanes, a new stress space is defined and the following definitions are required.

$$\varepsilon_V = \frac{\varepsilon_{kk}}{3} \tag{17}$$

$$\varepsilon_{Dev} = \sqrt{\varepsilon_D{}^2 + \varepsilon_M{}^2 + \varepsilon_L{}^2} \tag{18}$$

The volumetric strain component is similar to the previous definition and is the same for all microplanes. The deviatoric strain component is defined as the resultant of the normal strain component and the two shear components. Therefore, the stresses corresponding to the above strains are defined as follows:

$$\sigma_V = \frac{\sigma_{kk}}{3} \tag{19}$$

$$\sigma_{Dev} = \sqrt{\sigma_D{}^2 + \sigma_M{}^2 + \sigma_L{}^2} \tag{20}$$

According to Equations (15) to (20), the stress- strain relationship on the microplanes in the newly defined stress space is as follows:

$$\begin{aligned}d\varepsilon_V^{e(\mu)} &= \frac{1}{E_V}d\sigma_V^{(\mu)}\\ d\varepsilon_{Dev}^{e(\mu)} &= \frac{1}{E_T}d\sigma_{Dev}^{(\mu)}\end{aligned} \tag{21}$$

Soil plastic dilatation parameter for microplane $d_g^{(\mu)}$ is defined as follows:

$$d_g^{(\mu)} = \frac{d\varepsilon_V^{p(\mu)}}{d\varepsilon_{Dev}^{p(\mu)}} \tag{22}$$

It can be seen that $d_g^{(\mu)}$ in each microplane has a linear relationship with the stress ratio of that plane. Therefore, the dilatation of the microplanes is defined as follows:

$$d_g^{(\mu)} = \left(1+\alpha^{(\mu)}\right)\left(M_g^{(\mu)} - \eta^{(\mu)}\right) \quad , \quad \eta^{(\mu)} = \frac{d\sigma_{Dev}^{(\mu)}}{d\sigma_V^{(\mu)}} \tag{23}$$

Where $\alpha^{(\mu)}$ and $M_g^{(\mu)}$ are the constants of the model. The rate of plastic strain on the microplane is defined as follows:

$$d\varepsilon^{p(\mu)} = \lambda^{(\mu)}n_g^{(\mu)} \quad , \quad \lambda^{(\mu)} = \frac{1}{H^{(\mu)}}n^{(\mu)T}d\sigma^{(\mu)} \tag{24}$$

According to Figure 3, the unit vector normal to the plastic potential surface $n_g^{(\mu)}$, which shows the direction of plastic flow on the microplane (μ), is defined as follows:

$$
\begin{aligned}
&n_g^{(\mu)} = \left(n_{g-V}^{(\mu)}, n_{g-Dev}^{(\mu)}\right) \\
&n_{g-V}^{(\mu)} = \frac{d\varepsilon_V^{p\,(\mu)}}{\sqrt{\left(d\varepsilon_V^{p\,(\mu)}\right)^2 + \left(d\varepsilon_{Dev}^{p\,(\mu)}\right)^2}} = \frac{d_g^{(\mu)}}{\sqrt{1+\left(d_g^{(\mu)}\right)^2}} \\
&n_{g-Dev}^{(\mu)} = \frac{d\varepsilon_{Dev}^{p\,(\mu)}}{\sqrt{\left(d\varepsilon_V^{p\,(\mu)}\right)^2 + \left(d\varepsilon_{Dev}^{p\,(\mu)}\right)^2}} = \frac{1}{\sqrt{1+\left(d_g^{(\mu)}\right)^2}}
\end{aligned}
\tag{25}
$$

In a similar manner, the unit vector normal to the yield surface $n_f^{(\mu)}$ is defined as follows:

$$
\begin{aligned}
&n_f^{(\mu)} = \left(n_{f-V}^{(\mu)}, n_{f-Dev}^{(\mu)}\right) \\
&n_{f-V}^{(\mu)} = \frac{d_f^{(\mu)}}{\sqrt{1+\left(d_f^{(\mu)}\right)^2}} \\
&n_{f-Dev}^{(\mu)} = \frac{1}{\sqrt{1+\left(d_f^{(\mu)}\right)^2}}
\end{aligned}
\tag{26}
$$

$$
d_f^{(\mu)} = \left(1+\alpha_f^{(\mu)}\right)\left(M_f^{(\mu)} - \eta^{(\mu)}\right) \tag{27}
$$

where $\alpha_f^{(\mu)}$ and $M_f^{(\mu)}$ are the model constants. Therefore, by substituting Equations (25) and (26) in Equation (24), the plastic strain components on the microplanes are defined as follows

$$
\begin{aligned}
d\varepsilon_V^{p\,(\mu)} &= \frac{1}{H^{(\mu)}} n_{g-V}^{(\mu)}\, n_{f-V}^{(\mu)}\, d\sigma_V^{(\mu)} + \frac{1}{H^{(\mu)}} n_{g-V}^{(\mu)}\, n_{f-Dev}^{(\mu)}\, d\sigma_{Dev}^{(\mu)} \\
d\varepsilon_{Dev}^{p\,(\mu)} &= \frac{1}{H^{(\mu)}} n_{g-Dev}^{(\mu)}\, n_{f-V}^{(\mu)}\, d\sigma_V^{(\mu)} + \frac{1}{H^{(\mu)}} n_{g-Dev}^{(\mu)}\, n_{f-Dev}^{(\mu)}\, d\sigma_{Dev}^{(\mu)}
\end{aligned}
\tag{28}
$$

Plastic modulus $H^{(\mu)}$ of microplanes similar to the modulus used in the Pastor- Zienkiewicz model [35,36] for sand is defined as follows

$$
\begin{aligned}
&H^{(\mu)} = H_0^{(\mu)}\, \sigma_V^{(\mu)}\, H_f^{(\mu)} \left(H_v^{(\mu)} + H_s^{(\mu)}\right) H_{DM}^{(\mu)} \\
&H_f^{(\mu)} = \left(1 - \frac{\eta^{(\mu)}}{\eta_f^{(\mu)}}\right) \qquad , \qquad \eta_f^{(\mu)} = \left(1 + \frac{1}{\alpha_f^{(\mu)}}\right) M_f^{(\mu)} \\
&H_v^{(\mu)} = \left(1 - \frac{\eta^{(\mu)}}{M_g^{(\mu)}}\right) \\
&H_s^{(\mu)} = \beta_0^{(\mu)}\, \beta_1^{(\mu)} \exp\left(-\beta_0^{(\mu)}\, \xi^{(\mu)}\right) \qquad , \qquad \xi^{(\mu)} = \int \left| d\varepsilon_{Dev}^{p\,(\mu)} \right|
\end{aligned}
\tag{29}
$$

The coefficient $H_{DM}^{(\mu)}$ is introduced to take into account the stress history in cyclic loading and in over-consolidated clays and is defined as follows.

$$
H_{DM}^{(\mu)} = \left(\frac{\zeta_{Max}^{(\mu)}}{\zeta^{(\mu)}}\right)^{\gamma^{(\mu)}} \tag{30}
$$

The parameter $\zeta^{(\mu)}$ for the microplanes is defined as follows[37]

$$\zeta^{(\mu)} = \sigma_V^{(\mu)} \left[1 - \left(\frac{\alpha_f^{(\mu)}}{1+\alpha_f^{(\mu)}} \right) \frac{\eta^{(\mu)}}{M_f^{(\mu)}} \right]^{-1/\alpha_f^{(\mu)}} \tag{31}$$

For clays, the plastic modulus is defined as follows

$$H^{(\mu)} = H_0^{(\mu)} \sigma_V^{(\mu)} \left(f\left(\eta\right)^{(\mu)} + g\left(\xi\right)^{(\mu)} \right) H_{DM}^{(\mu)} \tag{32}$$

$$f\left(\eta\right)^{(\mu)} = \left[1 - \frac{\eta^{(\mu)}}{M^{(\mu)}} \right]^{\omega^{(\mu)}} \frac{\left[1 + \left(d_0^{(\mu)} \right)^2 \right]}{\left[1 + \left(d^{(\mu)} \right)^2 \right]} \left| sign\left[1 - \frac{\eta^{(\mu)}}{M^{(\mu)}} \right] \right| \tag{33}$$

$$\begin{aligned} d_0^{(\mu)} &= \left(1+\alpha^{(\mu)}\right) M^{(\mu)} \\ g\left(\xi\right)^{(\mu)} &= \beta^{(\mu)} \exp\left(-\beta^{(\mu)} \xi^{(\mu)}\right) \\ \beta^{(\mu)} &= \beta_0^{(\mu)} \left(1 - \frac{\zeta^{(\mu)}}{\zeta_{Max}^{(\mu)}} \right) \end{aligned} \tag{34}$$

And the plastic modulus during unloading is obtained from the following equation

$$\begin{aligned} H_u^{(\mu)} &= H_{u0}^{(\mu)} \left(\frac{M_g^{(\mu)}}{\eta_u^{(\mu)}} \right)^{\gamma_u^{(\mu)}} \qquad for \quad \left| \frac{M_g^{(\mu)}}{\eta_u^{(\mu)}} \right| > 1 \\ H_u^{(\mu)} &= H_{u0}^{(\mu)} \qquad\qquad\quad for \quad \left| \frac{M_g^{(\mu)}}{\eta_u^{(\mu)}} \right| > 1 \end{aligned} \tag{35}$$

where $\eta_u^{(\mu)}$ represents the stress ratio of microplane μ from which unloading has begun. $H_0^{(\mu)}, \beta_0^{(\mu)}, \beta_1^{(\mu)}, \omega^{(\mu)}, \gamma^{(\mu)}$ and $\gamma_u^{(\mu)}$ are the model constants.

The total strain rate for each microplane is equal to the sum of the elastic strain rate and the plastic strain rate. Thus, it could be written by adding Equations (21) and (28) as:

$$\begin{aligned} d\varepsilon_V^{(\mu)} &= d\varepsilon_V^{e(\mu)} + d\varepsilon_V^{p(\mu)} = \left(\frac{1}{E_V} + \frac{1}{H^{(\mu)}} n_{g-V}^{(\mu)} n_{f-V}^{(\mu)} \right) d\sigma_V^{(\mu)} + \frac{1}{H^{(\mu)}} n_{g-V}^{(\mu)} n_{f-Dev}^{(\mu)} d\sigma_{Dev}^{(\mu)} \\ d\varepsilon_{Dev}^{(\mu)} &= d\varepsilon_{Dev}^{e(\mu)} + d\varepsilon_{Dev}^{p(\mu)} = \frac{1}{H^{(\mu)}} n_{g-Dev}^{(\mu)} n_{f-V}^{(\mu)} d\sigma_V^{(\mu)} + \left(\frac{1}{E_T} + \frac{1}{H^{(\mu)}} n_{g-Dev}^{(\mu)} n_{f-Dev}^{(\mu)} \right) d\sigma_{Dev}^{(\mu)} \end{aligned} \tag{36}$$

Now, $d\sigma_V^{(\mu)}$ and $d\sigma_{Dev}^{(\mu)}$ are obtained by solving the system of Equation (36) for each microplane. q is a factor of $d\sigma_{Dev}^{(\mu)}$.

$$d\sigma_D^{(\mu)} = \frac{d\sigma_{Dev}^{(\mu)} . \left(\partial \sigma_D / \partial q \right)}{\sqrt{\left(\partial \sigma_D / \partial q \right)^2 + \left(\partial \sigma_M / \partial q \right)^2 + \left(\partial \sigma_L / \partial q \right)^2}} \tag{37}$$

$$d\sigma_M^{(\mu)} = \frac{d\sigma_{Dev}^{(\mu)} . \left(\partial \sigma_M / \partial q \right)}{\sqrt{\left(\partial \sigma_D / \partial q \right)^2 + \left(\partial \sigma_M / \partial q \right)^2 + \left(\partial \sigma_L / \partial q \right)^2}} \tag{38}$$

$$d\sigma_L^{(\mu)} = \frac{d\sigma_{Dev}^{(\mu)} . \left(\partial \sigma_L / \partial q \right)}{\sqrt{\left(\partial \sigma_D / \partial q \right)^2 + \left(\partial \sigma_M / \partial q \right)^2 + \left(\partial \sigma_L / \partial q \right)^2}} \tag{39}$$

$$\frac{\partial \sigma_D}{\partial q} = \frac{\partial \sigma_D}{\partial \sigma_{ij}} \cdot \frac{\partial \sigma_{ij}}{\partial q} = N_{ij} \frac{S_{ij}}{q} \tag{40}$$

$$\frac{\partial \sigma_M}{\partial q} = \frac{\partial \sigma_M}{\partial \sigma_{ij}} \cdot \frac{\partial \sigma_{ij}}{\partial q} = M_{ij} \frac{S_{ij}}{q} \tag{41}$$

$$\frac{\partial \sigma_L}{\partial q} = \frac{\partial \sigma_L}{\partial \sigma_{ij}} \cdot \frac{\partial \sigma_{ij}}{\partial q} = L_{ij} \frac{S_{ij}}{q} \tag{42}$$

In which, S_{ij} is the deviatoric stress tensor, $q = \sqrt{3J_2}$, and J_2 is the second invariant of stress tensor. Now, using Equations (7), (14) and (37) to (42), the stress tensor in the Cartesian space can be obtained.

3. Determination of the model constants

In general, model constants for different microplanes can have different values due to their strain history. Due to the lack of tests conducted on the 17 microplanes, all of them are assumed to have identical constants. These constants are determined using a sensitivity analysis [8]. In fact, the same value for each parameter is a weighted average of the value of that parameter on all planes. The constants used here for Banding sand and a sand represented by Taylor[38] at different relative densities are shown in

Table 2. Also, the constants of Bangkok clay and Weald clay are shown in

Table 3.

4. Simulations and results

In order to validate the performance of the proposed model, the results were compared with results predicted by generalized plasticity constitutive model[35] and laboratory data for several types of clay and sand in drained and undrained conditions. Two types of clay and two types of sand have been studied.

4-1 Bangkok clay

A series of tests have been carried out by Balasubramaniam and Chaudry[39] for undisturbed specimens of soft Bangkok clay. The undisturbed samples were taken at a depth of $5.5-6m$. The average index properties and natural water content are as follows: (1) Natural water content $=112\%-130\%$; (2) liquid limit $=118\%\pm 2\%$; (3) plastic limit $=43\%\pm 2\%$; and (4) plasticity index $=75\%\pm 4\%$. An undrained test was carried out on specimen isotropically consolidated to stress of $415kPa$ and a drained test was carried out on specimen isotropically consolidated to stress of $138kPa$. These specimens were subsequently sheared with increasing axial stress and under constant cell pressure.

Predictions of the drained and undrained triaxial compression tests, together with experimental results, and results presented by Pastor- Zienkiewicz (PZ) model[35] are shown in Figure 4 and Figure 5 respectively.

4-2 Weald clay

A series of triaxial compression tests on remoulded Weald clay was carried out by Henkel[40]. Weald clay is an estuarine deposit of the Cretaceous period, in the natural state heavily overconsolidated, with index properties $LL = 43\%$, $PL = 18\%$, $PI = 25\%$ and 40% fraction of clay minerals[40].

The results predicted by the model for both undrained and drained tests on normally consolidated specimens are compared with the data from the standard triaxial test under confining pressure of $30\ psi$ and results presented by Pastor- Zienkiewicz (PZ) model are shown in Figure 6.

For comparison, the results obtained on heavily overconsolidated specimens of Weald Clay, with an overconsolidation ratio of 24 under test cell pressure of $5\ psi$, are shown in Figure 7.

4-3 Banding sand

The results of a series of undrained triaxial tests on Bending sand are presented by Castro[41]. Four samples with relative densities of 64%, 47%, 44% and 29%, with initial void ratios of 0.639, 0.707, 0.719 and 0.786 respectively, were loaded with confining pressure of $392\ kPa$ in undrained conditions. The comparison of the predictions of the proposed model with the experimental data and the results provided by the PZ model[35] are shown in Figure 8.

4-4 Fort Peck sand

The experimental results of a sand in drained conditions and in two dense and loose states are presented by Taylor[38]. The triaxial drained test has been performed on two specimens with relative densities of 100% and 20%, with initial void ratios of 0.605 and 0.834, respectively, with confining pressure of $207\ kPa$.

The results of the proposed model together with the experimental data and the results of the PZ model are presented in Figure 9.

5. Conclusion

Philosophies of multilaminate approach and finite element combine well. While finite elements present a spatial discretization (with respect to distance), the multilaminate approach can be considered an angular discretization (related to the direction of different planes). In both methods, the principle of virtual work is used in similar ways, suitable for explicit temporal integration.

In this work, a new volumetric- deviatoric stress space is presented on the microplanes. In this stress space, the inherent simplicity of the model facilitates understanding and intuition in terms of the concept that is achieved by working with the stress and strain components on the microplanes instead of the tensors and their variables. It is important because it makes modeling complex materials easier. Using a multilaminate model causes the constitutive law to be written algebraically on the planes without using tensors. The stress tensor in the continuum is obtained by summing the effects of different planes. This model also avoids some of the other complexities associated with classical plasticity models, including that the yield and potential plastic surfaces are not explicitly defined. Despite the conceptual simplicity, it can be seen that this model has presented good predictions of material behavior for different materials and in different conditions.

The constitutive model presented in this paper can easily simulate the behavior of anisotropic materials using a multilaminate approach. In different directions where there is anisotropy, it is enough to use different model parameters or weight functions for planes related to the same directions.

The main limitation of the proposed model is that, similar to the PZ model[35], it does not enter the state parameter of the void ratio into constitutive relations, and the constants of the model are different for each initial void ratio. Of course, the model can be developed to consider state parameters, such as[37,42,43].

References

1. Zienkiewicz, O. C. and Pande, G. N., "Time- dependent multilaminate model of rocks—a numerical study of deformation and failure of rock masses", *Journal of International Journal for Numerical Analytical Methods in Geomechanics*, **1**(3), pp. 219–247 (1977). https://doi.org/10.1002/nag.1610010302

2. Pande, G. N. and Sharma, K. G., "Multi- laminate model of clays—a numerical evaluation of the influence of rotation of the principal stress axes", *International journal for numerical analytical methods in geomechanics*, **7**(4), pp. 397–418 (1983). https://doi.org/10.1002/nag.1610070404

3. Shiomi, T. and Pietruszczak, S., "A liquefaction study of sand layers using the reflecting surface model" (1982).

4. Bažant, Z. P. and Oh, B. H., "Crack band theory for fracture of concrete", *Matériaux et construction*, **16**, pp. 155–177 (1983). https://doi.org/10.1007/BF02486267

5. Sadrnejad, S. A. and Pande, G. N., "A multilaminate model for sands", *numerical models in geomechanics* (1989). https://doi.org/10.1016/0148-9062(90)91299-M

6. Sadrnejad, S. A., Daryan, A. S., and Ziaei, M., "A constitutive model for multi-line simulation of granular material behavior using multi-plane pattern", *Journal of Computer Science*, **5**(11), p. 822 (2009). http://dx.doi.org/10.3844/jcssp.2009.822.830

7. Zreid, I. and Kaliske, M., "An implicit gradient formulation for microplane Drucker-Prager plasticity", *Int J Plast*, **83**, pp. 252–272 (2016). https://doi.org/10.1016/j.ijplas.2016.04.013

8. Dashti, H., Sadrnejad, S. A., and Ganjian, N., "A novel semi-micro multilaminate elasto-plastic model for the liquefaction of sand", *Soil Dynamics and Earthquake Engineering*, **124**, pp. 121–135 (2019). https://doi.org/10.1016/j.soildyn.2019.05.031

9. Dafalias, Y. F. and Manzari, M. T., "Simple plasticity sand model accounting for fabric change effects", *J Eng Mech*, **130**(6), pp. 622–634 (2004). https://doi.org/10.1061/(ASCE)0733-9399(2004)130:6(622)

10. Malisetty, R. S., Indraratna, B., and Vinod, J. S., "Multilaminate mathematical framework for analyzing the deformation of coarse granular materials", *International Journal of Geomechanics*, **20**(6), p. 6020004 (2020). https://doi.org/10.1061/(ASCE)GM.1943-5622.0001669

11. Dadgar, H. R., Arjomand, M. A., and Arefnia, A., "Numerical analysis of cyclic loading effect on progressive failure of an earth dam upon a multi-laminate framework", *Soils and Rocks*, **44**, p. e2021056720 (2021). http://dx.doi.org/10.28927/SR.2021.056720

12. Galavi, V. and Schweiger, H. F., "Nonlocal multilaminate model for strain softening analysis", *International Journal of Geomechanics*, **10**(1), pp. 30–44 (2010). https://doi.org/10.1061/(ASCE)1532-3641(2010)10:1(30)

13. Malisetty, R. S., Indraratna, B., and Vinod, J., "Behaviour of ballast under principal stress rotation: Multi-laminate approach for moving loads", *Comput Geotech*, **125**, p. 103655 (2020). https://doi.org/10.1016/j.compgeo.2020.103655

14. Saleem, M., "Microplane modeling of the elasto-viscoplastic constitution", *Journal of Research in Science, Engineering Technology*, **8**(3), pp. 19–25 (2020). https://doi.org/10.24200/jrset.vol8iss3pp19-25

15. Schädlich, B. and Schweiger, H. F., "Influence of anisotropic small strain stiffness on the deformation behavior of geotechnical structures", *International Journal of Geomechanics*, **13**(6), pp. 861–868 (2013). https://doi.org/10.1061/(ASCE)GM.1943-5622.0000286

16. Sadrnejad, S. A. and Shakeri, S., “Multi-laminate non-coaxial modelling of anisotropic sand behavior through damage formulation”, *Comput Geotech*, **88**, pp. 18–31 (2017). https://doi.org/10.1016/j.compgeo.2017.02.018

17. Dashti, H., Sadrnejad, S. A., and Ganjian, N., “Multi-directional modeling for prediction of fabric anisotropy in sand liquefaction”, *Comput Geotech*, **92**, pp. 156–168 (2017). https://doi.org/10.1016/j.compgeo.2017.08.002

18. Dashti, H., Sadrnejad, S. A., and Ganjian, N., “Modification of a constitutive model in the framework of a multilaminate method for post-liquefaction sand”, *Latin American Journal of Solids and Structures*, **14**, pp. 1569–1593 (2017). https://doi.org/10.1590/1679-78253841

19. Pietruszczak, S. and Pande, G. N., “Description of soil anisotropy based on multi- laminate framework”, *Int J Numer Anal Methods Geomech*, **25**(2), pp. 197–206 (2001). https://doi.org/10.1002/nag.125

20. Sadrnejad, S. A. and Karimpour, H., “Drained and undrained sand behaviour by multilaminate bounding surface model”, *International Journal of Civil Engineering*, **9**(2), pp. 111–125 (2011). http://ijce.iust.ac.ir/article-1-366-en.html

21. Tavanaeifar, H. and Akhaveissy, A. H., “3D Continuous Micro-Model Based on Multi-laminate Concept for the Nonlinear Numerical Analysis of Masonry Panels”, *Amirkabir Journal of Civil Engineering*, **53**(11), pp. 4969–4988 (2022). https://doi.org/10.22060/ceej.2021.18672.6920

22. Sadrnejad, S. A. and Hoseinzadeh, M. R., “Multi-laminate rate-dependent modelling of static and dynamic concrete behaviors through damage formulation”, *Scientia Iranica*, **26**(3), pp. 1194–1205 (2019). https://doi.org/10.24200/sci.2017.4581

23. Bayraktaroglu, H., Hicks, M. A., Korff, M., and Galavi, V., “A state-dependent multilaminate constitutive model for anisotropic sands”, *Géotechnique*, pp. 1–17 (2023). https://doi.org/10.1680/jgeot.22.00165

24. Bažant, Z. P., Caner, F. C., Carol, I., Adley, M. D., and Akers, S. A., “Microplane model M4 for concrete. I: Formulation with work-conjugate deviatoric stress”, *J Eng Mech*, **126**(9), pp. 944–953 (2000). https://doi.org/10.1061/(ASCE)0733-9399(2000)126:9(944)

25. Caner, F. C., de Carlos Blasco, V., and Egido, M. G., “Microplane Models for Elasticity and Inelasticity of Engineering Materials”, In *Handbook of Nonlocal Continuum Mechanics for Materials and Structures*, G. Z. Voyiadjis, Ed., Springer International Publishing, Cham, pp. 1065–1097 (2019). https://doi.org/10.1007/978-3-319-22977-5_1-1

26. Cudny, M. and Vermeer, P. A., “On the modelling of anisotropy and destructuration of soft clays within the multi-laminate framework”, *Comput Geotech*, **31**(1), pp. 1–22 (2004). https://doi.org/10.1016/j.compgeo.2003.12.001

27. Sadrnezhad, S., “Constitutive model for multi-laminate induced anisotropic double hardening elastic-plasticity of sand” (2002). https://civilica.com/doc/1415744

28. Bažant, Z. P. and Prat, P. C., “Microplane model for brittle-plastic material: II. Verification”, *J Eng Mech*, **114**(10), pp. 1689–1702 (1988). https://doi.org/10.1061/(ASCE)0733-9399(1988)114:10(1689)

29. Bažant, Z. P. and Prat, P. C., “Microplane model for brittle-plastic material: I. Theory”, *J Eng Mech*, **114**(10), pp. 1672–1688 (1988). https://doi.org/10.1061/(ASCE)0733-9399(1988)114:10(1672)

30. Bazant, Z. P., “MICROPLANE MODEL FOR STRAIN-CONTROLLED INELASTIC BEHAVIOUR”, In *Unknown Host Publication Title*, John Wiley & Sons, pp. 45–59 (1984).

31. Bažant, Z. P., Xiang, Y., and Prat, P. C., “Microplane model for concrete. I: Stress-strain boundaries and finite strain”, *J Eng Mech*, **122**(3), pp. 245–254 (1996). https://doi.org/10.1061/(ASCE)0733-9399(1996)122:3(245)

32. Bažant, P. and Oh, B. H., “Efficient numerical integration on the surface of a sphere”, *ZAMM - Journal of Applied Mathematics and Mechanics/Zeitschrift für Angewandte Mathematik und Mechanik*, **66**(1), pp. 37–49 (1986). https://doi.org/10.1002/zamm.19860660108

33. Stroud, A. H., *Approximate Calculation of Multiple Integrals*, Prentice Hall (1971). https://doi.org/10.2307/2005635

34. Bažant, Z. P. and Oh, B. H., “Microplane model for progressive fracture of concrete and rock”, *J Eng Mech*, **111**(4), pp. 559–582 (1985). https://doi.org/10.1061/(ASCE)0733-9399(1985)111:4(559)

35. Pastor, M., Zienkiewicz, O. C., and Chan, A. H. C., “Generalized plasticity and the modelling of soil behaviour”, *Int J Numer Anal Methods Geomech*, **14**(3), pp. 151–190 (1990). https://doi.org/10.1002/nag.1610140302

36. Zienkiewicz, O. C., Leung, K. H., and Pastor, M., “Simple model for transient soil loading in earthquake analysis. I. Basic model and its application”, *Int J Numer Anal Methods Geomech*, **9**(5), pp. 453–476 (1985). https://doi.org/10.1002/nag.1610090505

37. Manzanal, D., Fernández Merodo, J. A., and Pastor, M., “Generalized plasticity state parameter-based model for saturated and unsaturated soils. Part 1: Saturated state”, *Int J Numer Anal Methods Geomech*, **35**(12), pp. 1347–1362 (2011). https://doi.org/10.1002/nag.961

38. Taylor, D. W., *Fundamentals of Soil Mechanics*, LWW (1948). https://doi.org/10.1097/00010694-194808000-00008

39. Balasubramaniam, A. S. and Chaudry, A. R., “Deformation and strength characteristics of soft Bangkok clay”, *Journal of the Geotechnical Engineering Division*, **104**(9), pp. 1153–1167 (1978). https://doi.org/10.1061/AJGEB6.0000685

40. Henkel, D. J., “The effect of overconsolidation on the behaviour of clays during shear”, *Géotechnique*, **6**(4), pp. 139–150 (1956). https://doi.org/10.1680/geot.1956.6.4.139

41. Castro, G., “Liquefaction of sands”, *Ph. D. Thesis, Harvard University, Mass* (1969).

42. Ling, H. I. and Yang, S., “Unified sand model based on the critical state and generalized plasticity”, *J Eng Mech*, **132**(12), pp. 1380–1391 (2006). https://doi.org/10.1061/(ASCE)0733-9399(2006)132:12(1380)

43. Heidarzadeh, H. and Oliaei, M., “Development of a generalized model using a new plastic modulus based on bounding surface plasticity”, *Acta Geotech*, **13**, pp. 925–941 (2018). https://doi.org/10.1007/s11440-017-0599-0

44. Sadrnejad, S. A. and Shakeri, S., “Fabric assessment of damaged anisotropic geo-materials using the multi-laminate model”, *International Journal of Rock Mechanics and Mining Sciences*, **91**, pp. 90–103 (2017). https://doi.org/10.1016/j.ijrmms.2016.11.013

45. SADRNEZHAD, S., “A general multi-plane model for post-liquefaction of sand” (2007). https://doi.org/10.22099/IJSTC.2007.736

List of figure captions:

Figure 1. (a) The position of the planes on the sphere (b) simulation of the sphere with planes[16,18]

Figure 2. components of strain on the microplane[24]

Figure 3. Typical yield and plastic potential surfaces of defined stress space on microplane and their unit normal vectors of them

Figure 4. Drained compression test on normally consolidated samples of Bangkok clay. Experimental data by Balasubramaniam and Chaudry[39] compared with predictions by the proposed and PZ[35] models

Figure 5. Undrained compression test on normally consolidated samples of Bangkok clay. Experimental data by Balasubramaniam and Chaudry[39] compared with predictions by the proposed and PZ[35] models

Figure 6. Drained and undrained compression tests on normally consolidated samples of Weald clay. Experimental data by Henke[40] compared with predictions by the proposed and PZ[35] models

Figure 7. Drained and undrained compression tests on overconsolidated samples with OCR=24 of Weald clay. Experimental data by Henkel[40] compared with predictions by the proposed and PZ[35] models

Figure 8. Undrained triaxial tests on Banding sand and their representation by the proposed and PZ[35] models. Experimental data from Castro[41]

Figure 9 Drained triaxial tests on a sand represented by Taylor[38] compared with predictions by the proposed and PZ[35] models

List of table captions:

Table 1. Direction cosines and weight coefficients of 17 planes[44,45]

Table 2. Model constants for Banding sand and a sand provided by Taylor for different densities

Table 3. Model constants for Bangkok and Weald clays

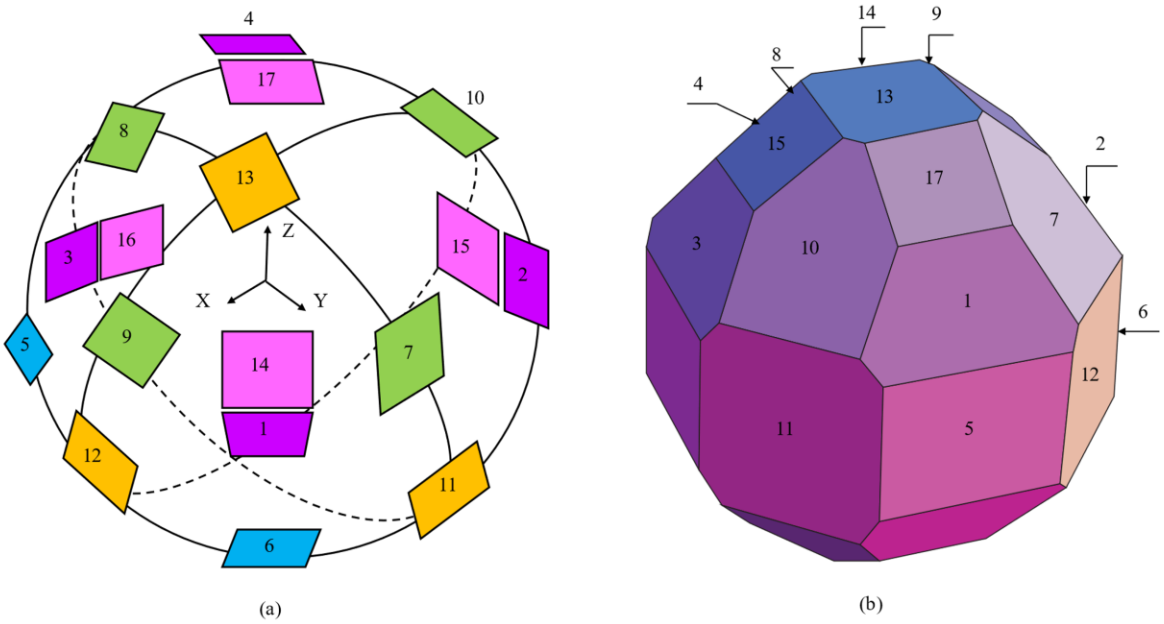

Figure 1.

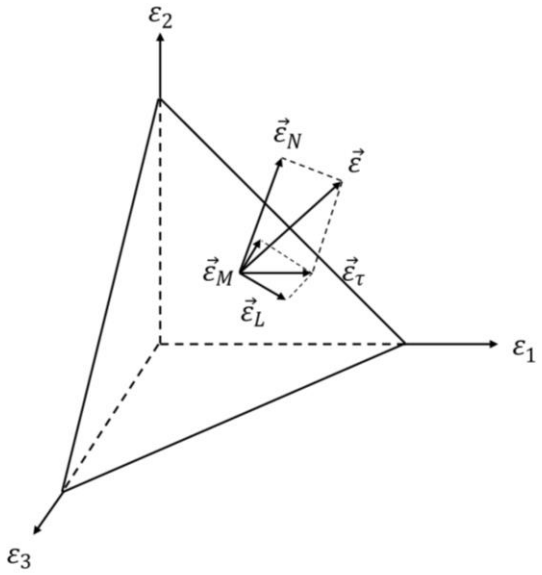

Figure 2.

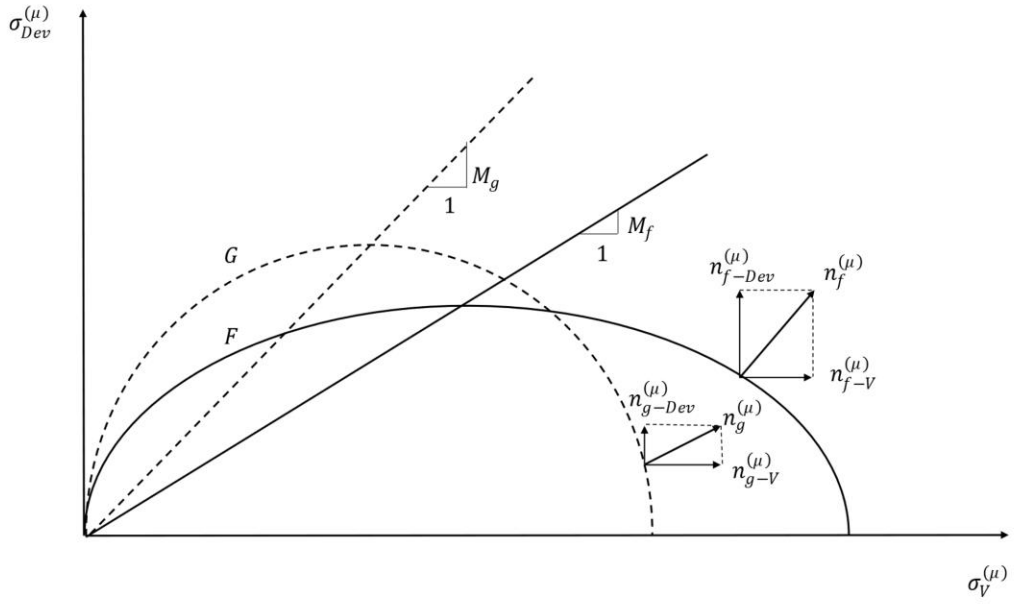

Figure 3.

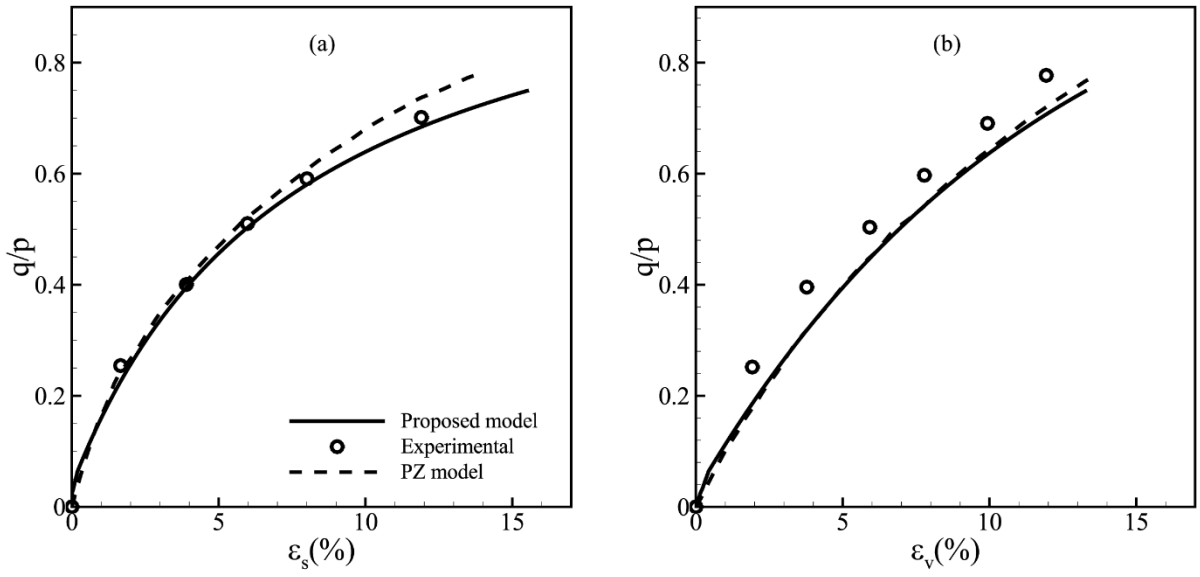

Figure 4.

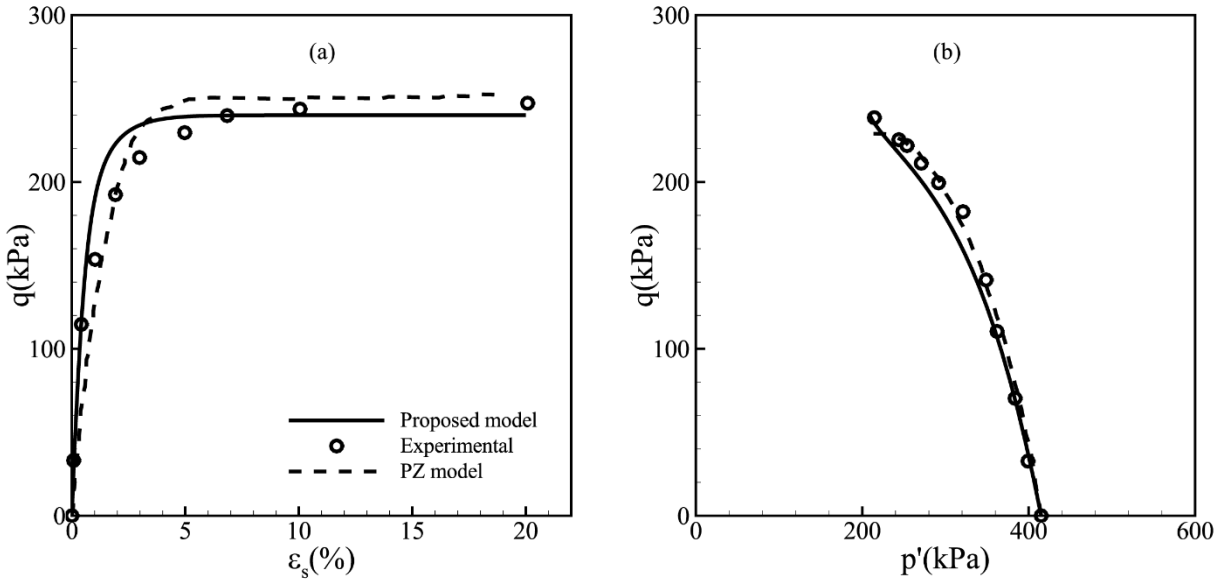

Figure 5.

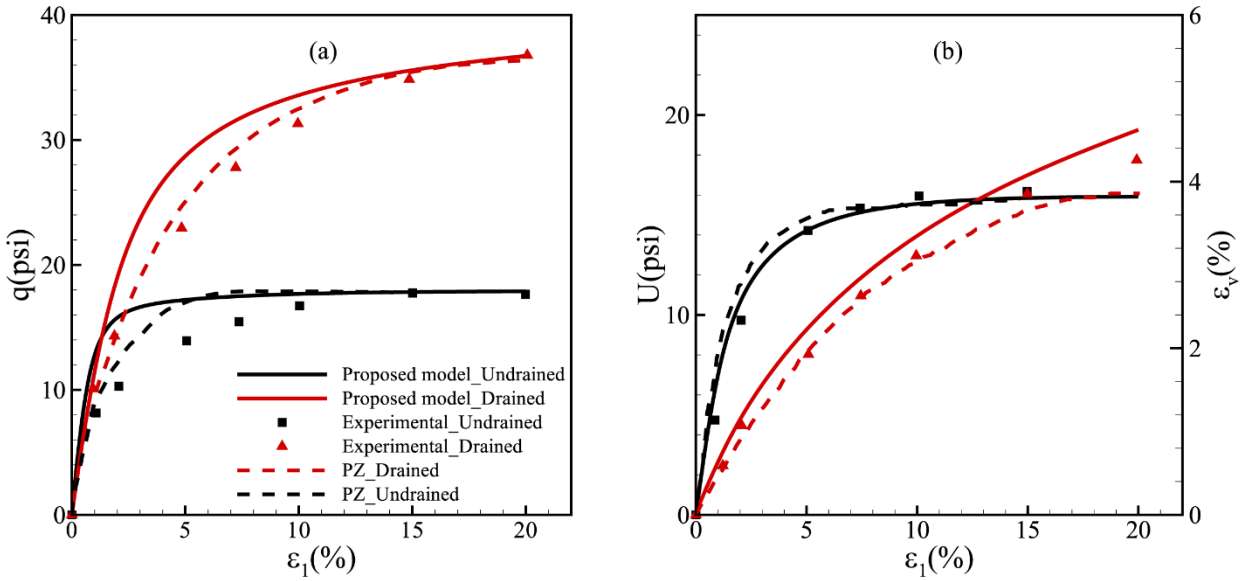

Figure 6.

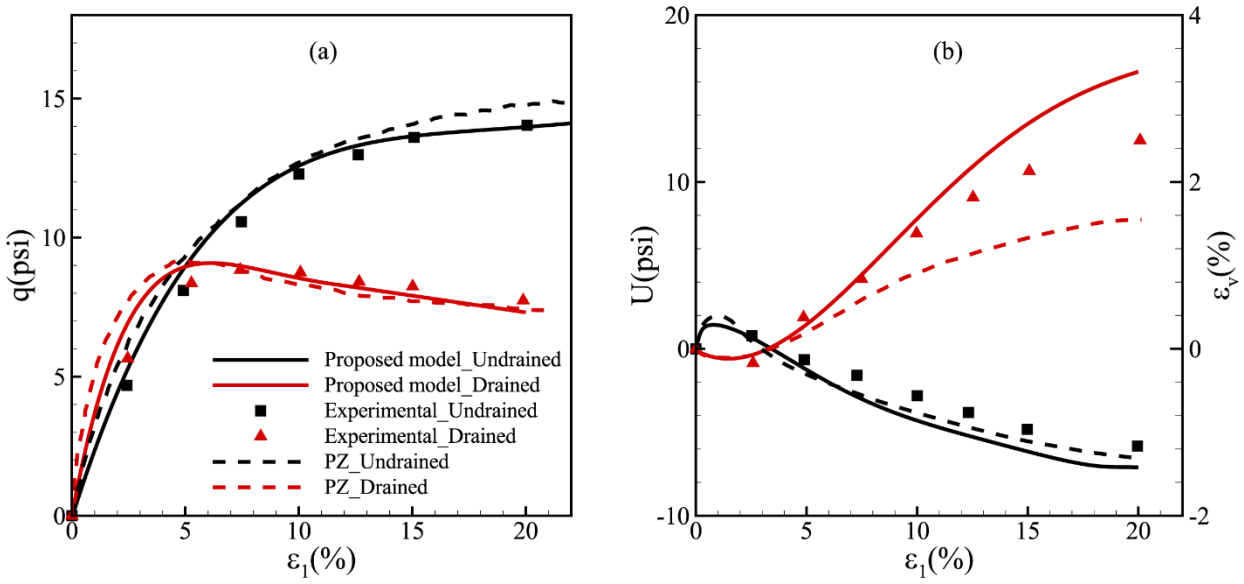
(a)
q(psi)
ε_1(%)
Proposed model_Undrained
Proposed model_Drained
Experimental_Undrained
Experimental_Drained
PZ_Undrained
PZ_Drained
(b)
U(psi)
ε_v(%)
ε_1(%)

Figure 7.

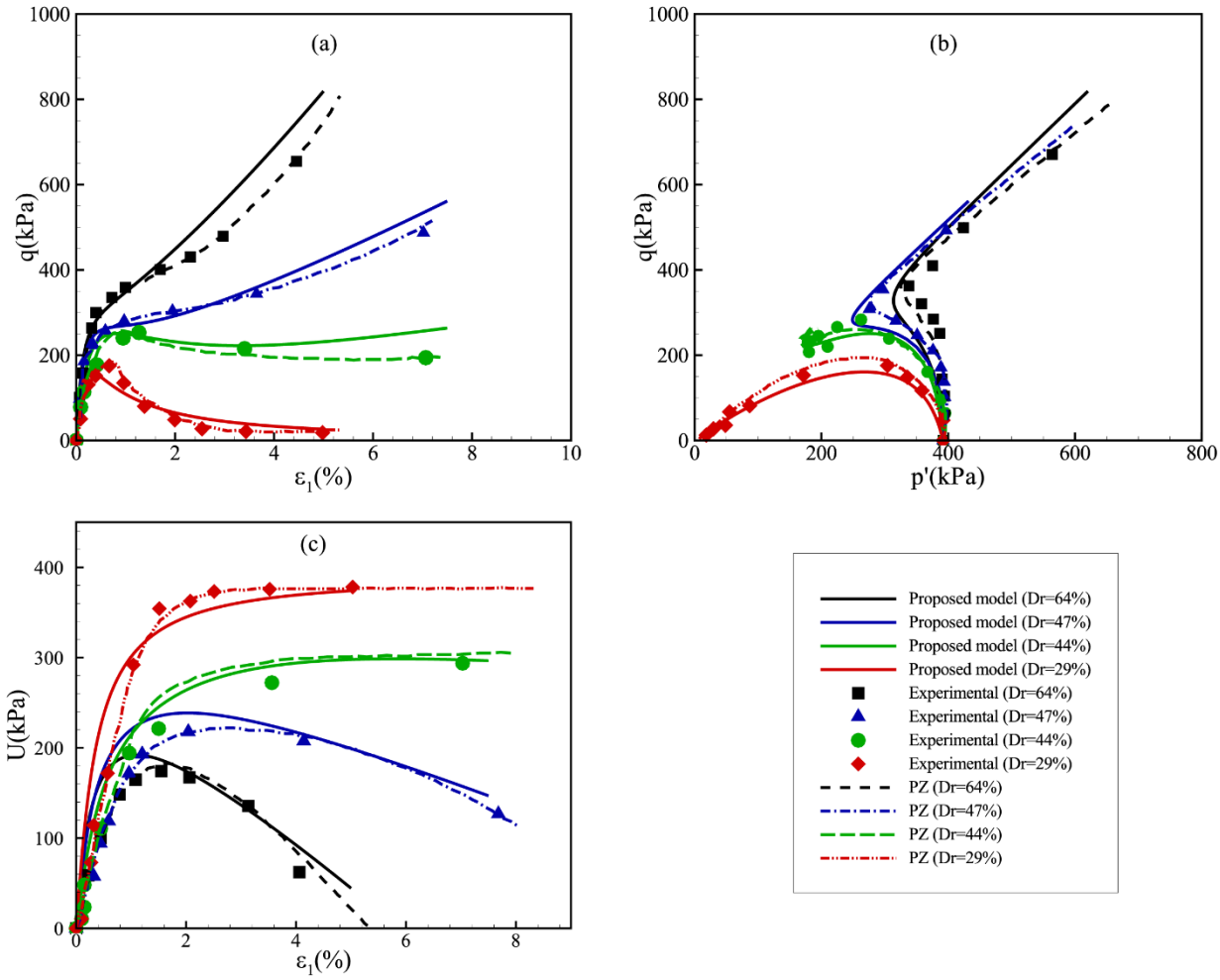
(a)
q(kPa)
ε1(%)
(b)
q(kPa)
p'(kPa)
(c)
U(kPa)
ε1(%)
Proposed model (Dr=64%)
Proposed model (Dr=47%)
Proposed model (Dr=44%)
Proposed model (Dr=29%)
Experimental (Dr=64%)
Experimental (Dr=47%)
Experimental (Dr=44%)
Experimental (Dr=29%)
PZ (Dr=64%)
PZ (Dr=47%)
PZ (Dr=44%)
PZ (Dr=29%)

Figure 8.

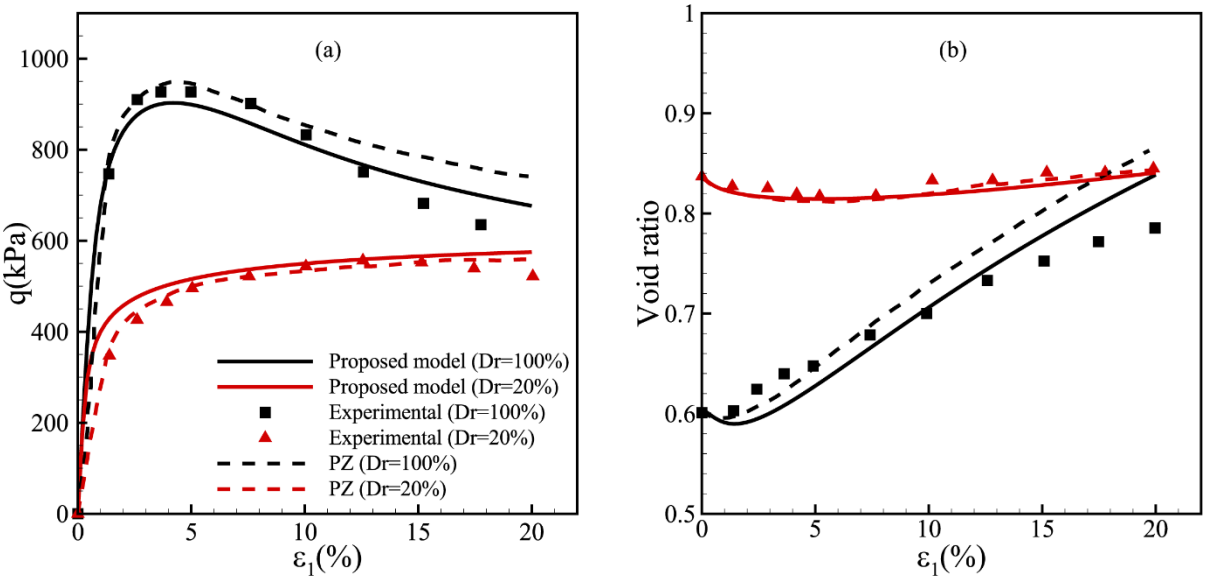

Figure 9.

Table 1.

Plane no.	$n_1^{(\mu)}$	$n_2^{(\mu)}$	$n_3^{(\mu)}$	$m_1^{(\mu)}$	$m_2^{(\mu)}$	$m_3^{(\mu)}$	$l_1^{(\mu)}$	$l_2^{(\mu)}$	$l_3^{(\mu)}$	$W^{(\mu)}$
1	$1/\sqrt{3}$	$1/\sqrt{3}$	$1/\sqrt{3}$	$1/\sqrt{2}$	$-1/\sqrt{2}$	*0*	$-1/\sqrt{6}$	$-1/\sqrt{6}$	$\sqrt{2/3}$	*0.020277985*
2	$1/\sqrt{3}$	$-1/\sqrt{3}$	$1/\sqrt{3}$	$-1/\sqrt{2}$	$-1/\sqrt{2}$	*0*	$-1/\sqrt{6}$	$1/\sqrt{6}$	$\sqrt{2/3}$	*0.020277985*
3	$-1/\sqrt{3}$	$1/\sqrt{3}$	$1/\sqrt{3}$	$1/\sqrt{2}$	$1/\sqrt{2}$	*0*	$1/\sqrt{6}$	$-1/\sqrt{6}$	$\sqrt{2/3}$	*0.020277985*
4	$-1/\sqrt{3}$	$-1/\sqrt{3}$	$1/\sqrt{3}$	$-1/\sqrt{2}$	$-1/\sqrt{2}$	*0*	$1/\sqrt{6}$	$1/\sqrt{6}$	$\sqrt{2/3}$	*0.020277985*
5	$1/\sqrt{2}$	$1/\sqrt{2}$	*0*	$1/\sqrt{2}$	$-1/\sqrt{2}$	*0*	*0*	*0*	*1*	*0.058130468*
6	$-1/\sqrt{2}$	$1/\sqrt{2}$	*0*	$1/\sqrt{2}$	$1/\sqrt{2}$	*0*	*0*	*0*	*1*	*0.058130468*
7	$1/\sqrt{2}$	*0*	$1/\sqrt{2}$	*0*	*-1*	*0*	$-1/\sqrt{2}$	*0*	$1/\sqrt{2}$	*0.030091134*
8	$-1/\sqrt{2}$	*0*	$1/\sqrt{2}$	*0*	*1*	*0*	$1/\sqrt{2}$	*0*	$1/\sqrt{2}$	*0.030091134*
9	*0*	$1/\sqrt{2}$	$1/\sqrt{2}$	*1*	*0*	*0*	*0*	$-1/\sqrt{2}$	$1/\sqrt{2}$	*0.030091134*
10	*0*	$-1/\sqrt{2}$	$1/\sqrt{2}$	*-1*	*0*	*0*	*0*	$1/\sqrt{2}$	$1/\sqrt{2}$	*0.030091134*
11	*1*	*0*	*0*	*0*	*-1*	*0*	*0*	*0*	*1*	*0.038296881*
12	*0*	*1*	*0*	*1*	*0*	*0*	*0*	*0*	*1*	*0.038296881*
13	*0*	*0*	*1*	*1*	*0*	*0*	*0*	*-1*	*0*	*0.0293006*
14	$1/\sqrt{6}$	$1/\sqrt{6}$	$\sqrt{2/3}$	$1/\sqrt{2}$	$-1/\sqrt{2}$	*0*	$-1/\sqrt{3}$	$-1/\sqrt{3}$	$1/\sqrt{3}$	*0.019070616*
15	$1/\sqrt{6}$	$-1/\sqrt{6}$	$\sqrt{2/3}$	$-1/\sqrt{2}$	$-1/\sqrt{2}$	*0*	$-1/\sqrt{3}$	$1/\sqrt{3}$	$1/\sqrt{3}$	*0.019070616*
16	$-1/\sqrt{6}$	$1/\sqrt{6}$	$\sqrt{2/3}$	$1/\sqrt{2}$	$1/\sqrt{2}$	*0*	$1/\sqrt{3}$	$-1/\sqrt{3}$	$1/\sqrt{3}$	*0.019070616*
17	$-1/\sqrt{6}$	$-1/\sqrt{6}$	$\sqrt{2/3}$	$-1/\sqrt{2}$	$1/\sqrt{2}$	*0*	$1/\sqrt{3}$	$1/\sqrt{3}$	$1/\sqrt{3}$	*0.019070616*

Table 2.

	from Taylor $(Dr = 20\%)$	from Taylor $(Dr = 100\%)$	Banding sand $(Dr = 29\%)$	Banding sand $(Dr = 44\%)$	Banding sand $(Dr = 47\%)$	Banding sand $(Dr = 64\%)$
$K_{ev0}^{(\mu)}(kPa)$	*30000*	*30000*	*35000*	*35000*	*35000*	*35000*
$G_{es0}^{(\mu)}(kPa)$	*50000*	*50000*	*52500*	*52500*	*52500*	*65000*
$M_f^{(\mu)}$	*0.26*	*0.36*	*0.217*	*0.255*	*0.264*	*0.333*
$M_g^{(\mu)}$	*0.69*	*0.65*	*0.661*	*0.6*	*0.518*	*0.476*
$H_0^{(\mu)}$	*4000*	*16000*	*350*	*350*	*350*	*350*
$\beta_0^{(\mu)}$	*0.133*	*0.133*	*0.133*	*0.133*	*0.133*	*0.133*
$\beta_1^{(\mu)}$	*3.39*	*3.39*	*6.326*	*6.326*	*6.326*	*6.326*
$\alpha^{(\mu)}$	*0.45*	*0.45*	*0.45*	*0.44*	*0.50*	*0.56*

Table 3.

	Weald clay	Bangkok clay
$K_{ev0}^{(\mu)}$	*766 (psi)*	*12420 (kPa)*
$G_{es0}^{(\mu)}$	*800 (psi)*	*15000 (kPa)*
$M^{(\mu)}$	*0.46*	*0.53*
$H_0^{(\mu)}$	*165*	*6.6*
$\omega^{(\mu)}$	*3*	*2*
$\beta_0^{(\mu)}$	*0.1*	-
$\gamma^{(\mu)}$	*0.4*	-
$\alpha^{(\mu)}$	*0.45*	*1.1*

Biographies:

Mohammad Falahatpour is currently a PhD student in Geotechnical Engineering, Tarbiat Modares University, Tehran, Iran. He received her MSc degree in Geotechnical Engineering from K.N Toosi University of Technology, Tehran, Iran, and his BS degree in Civil Engineering from Jundi-Shapur University of Technology, Dezful, Khuzestan, Iran. Her research interests include constitutive modeling of geotechnical material and numerical modeling.

Mohammad Oliaei is Assistant Professor of Civil Engineering. Since 2008, he joined the geotechnical group in the Department of Civil Engineering, Tarbiat Modares University. He received his PhD degree from Sharif University of Technology (2007) as first rank student. In 2005, he was awarded a scholarship from British Council to continue

his PhD study at Cambridge University. He specializes in the area of Geotechnical Engineering and Numerical Modeling. He is the reviewer of several ISI and Scientic & Technical Journals.

Heisam Heidarzadeh currently works at Shahrekord university. Heisam does research in Geotechnical Engineering / Civil Engineering. He is a faculty member in the department of civil engineering at Shahrekord University. The main area studied by Heidarzadeh is soil behavior models. He studies the behavior of soil plastics under different loads. However, he also studies such as dynamic analysis, structural control, and optimization. Heidarzadeh is also interested in various methods of nonlinear analysis.